J. Phys. II France **6** (1996) 1615–1638 NOVEMBER **1996**, PAGE 1615

Topological Characterization of Reconstructed Attractors Modding Out Symmetries

C. Letellier (*) and G. Gouesbet

Laboratoire d'Énergétique des Systèmes et Procédés (**), INSA de Rouen, B.P. 08, 76131 Mont-Saint-Aignan, France

(Received 24 October 1995, revised 2 May 1996, accepted 8 August 1996)

PACS.05.45.+b – Theory and models of chaotic systems

Abstract. — Topological characterization is important in understanding the subtleties of chaotic behaviour. Unfortunately it is based on the knot theory which is only efficiently developed in 3D spaces (namely $\mathbb{R}^3$ or in its one-point compactification S^3). Consequently, to achieve topological characterization, phase portraits must be embedded in 3D spaces, *i.e.* in a lower dimension than the one prescribed by Takens' theorem. Investigating embedding in low-dimensional spaces is, therefore, particularly meaningful. This paper is devoted to tridimensional systems which are reconstructed in a state space whose dimension is also 3. In particular, an important case is when the system studied exhibits symmetry properties, because topological properties of the attractor reconstructed from a scalar time series may then crucially depend on the variable used. Consequently, special attention is paid to systems with symmetry properties in which specific procedures for topological characterization are developed. In these procedures, all the dynamics are projected onto a so-called fundamental domain, leading us to the introduction of the concept of restricted topological equivalence, *i.e.* two attractors are topologically equivalent in the restricted sense, if the topological properties of their fundamental domains are the same. In other words, the symmetries are moded out by projecting the whole phase space onto a fundamental domain.

1. Introduction

State space reconstruction is the creation of multidimensional state space from a scalar time series. It is a prerequisite step for analyzing the behaviour of a dynamical system of which only one time series is known. A pioneering paper by Packard *et al.* [1] proposed two ways of reconstructing a state space, *i.e.* by using time delay or time derivative coordinates. Another kind of coordinate, namely principal components [2], is now commonly used. Gibson *et al.* [3] showed that the relationship between delays, derivatives and principal components consists in a rotation and a rescaling. Consequently, from Gibson's point of view, statements about the nature of the equivalence between the original phase portrait and the reconstructed one would be independent of the coordinate system. They may however depend on the reconstruction parameters. For instance, if one uses delay coordinates, it may be observed that the shape of a bounded manifold changes as the delay is changed [4], and at some point this manifold

(*) Author for correspondence (e-mail: letellie@coria.fr)
(**) URA CNRS 230

undergoes self intersections in the interior of which the flow appears to be constrained. Nevertheless, it is expected that there must exist a delay range for which a reconstructed attractor with delay coordinates is topologically equivalent to a reconstructed attractor with derivative coordinates. A study of this issue, although useful, will be postponed to future work.

Initially, only the phase portrait was reconstructed, allowing the study of the topological structure of the strange attractor and the determination of important global parameters such as fractal dimensions, Lyapunov exponents, *etc.* Another way of reconstructing state spaces is by using global vector field reconstructions. Indeed, for experimental systems, given a scalar time series for an observable, an important problem is to provide a set of ordinary differential equations equivalent to the original underlying system. There is a great deal of interest in this problem [4–12]. An equivalent reconstructed vector field may be an important step in gaining a better understanding of the underlying physical processes responsible for the chaos observed.

When a state space or a vector field is reconstructed, a question arises: is the reconstructed dynamics equivalent to the original dynamics? And more precisely, in which sense is it equivalent, *i.e.* how equivalent can it be? This is the basic question addressed in this paper for the special case of equivariant vector fields.

Takens [15] proved that in the absence of noise it is always possible to embed a time series in a state space. To ensure with probability one that a reconstruction is an embedding, *i.e.* that there exists a diffeomorphism from the original state space to the embedding space, the embedding dimension has to be $d_E \geq 2D_H + 1$ where D_H would ideally refer to the Haussdorff dimension of the attractor studied. If not, the diffeomorphism is not ensured but is quite possible. Indeed, diffeomorphisms between manifolds of the same dimension are not uncommon. Unfortunately Takens' theorem may be too demanding for experimentalists because it requires work in high-dimensional spaces. Indeed, the smaller the dimension of an embedding, the better the situation for analyzing the data. Thus, in spite of Takens' theorem, the choice of the embedding dimension is still a topic of particular interest [16–18]. Actually, Takens' theorem does not refer to cases when the dimension of the reconstructed state space is smaller than $2D_H + 1$. Such cases, however, are particularly important since topological characterization of attractors is based on the knot theory which is related to three dimensional spaces. Thus, topological characterization is always achieved with a lower dimension than the one defined by the Takens criterion.

The general purpose of the present paper is therefore to clarify the nature of equivalence between original and reconstructed attractors in 3D state spaces such as those presented in references [2, 5, 14], in the particular case concerning equivariant systems as exemplified by the Lorenz system [19]. The results of this paper are obtained with derivatives, which have the advantage of providing algebraic relationships between original and reconstructed spaces. Another advantage of derivatives is that global vector field reconstruction may be achieved in principle by working with a small piece of trajectory. For example, an attractor may be reconstructed by studying transients, or intermittency behaviour may be reconstructed by analyzing only laminar phases [20].

In the course of this study, specific procedures to perform the topological characterization of systems with symmetry properties (such as the Lorenz system) are developed. In such symmetrical systems we show that a fundamental domain is conveniently defined to characterize the topology of their related attractors. Indeed, we will show in this paper that the topology of the fundamental domain is of great importance in characterizing the dynamical behaviour of an equivariant system. In this approach, the topological characterization takes into account the symmetry to provide a description which acts independently of symmetry properties. In this way, a characterization may be obtained, even if the symmetry is not preserved by the reconstruction method, since we mod out the symmetry in the topological characterization.

Such a procedure is found to be useful when a dynamical system displaying some symmetries is reconstructed from a scalar time series since an attractor induced by a time series need not have the same symmetry properties. As a result, topological characterization of the original and reconstructed attractors may lead to two different templates, even though the underlying system is the same. Therefore, factoring out symmetry groups using concepts such as the fundamental domain is essential for carrying out a characterization independent of the choice of a particular embedding. The existence of a fundamental domain in which all the trajectory is projected leads us to introduce a procedure for topological characterization in this domain by using linking numbers counted on a plane projection and a fundamental template synthesizing the topological properties of the fundamental domain. We therefore introduce the concept of restricted topological equivalence meaning topological equivalence of related fundamental domains (and thus of related templates).

The paper is organized as follows. Section 2 is a brief review of the time derivative coordinate systems used to obtain reconstructed state spaces. When the original system is known, an algebraic transformation between original and reconstructed coordinates is obtained. A brief review of the topological characterization procedure is given thereafter. Section 3 is the main purpose of our paper. Successively, we show that i) the attractor reconstructed from the y-variable of the Rössler system is diffeomorphically equivalent to the original one and ii) the attractors reconstructed from the variables of the Lorenz system are topologically equivalent to the original one in fundamental domains but with different symmetry properties (consequences for the dynamical analysis from each variable are explained). This means that topological equivalence *stricto sensu* is not satisfied but restricted topological equivalence is nevertheless ensured. Section 4 is a conclusion.

2. Theoretical Background

2.1. Reconstruction Method. — Let us consider a time continuous dynamical system defined by a set of ordinary differential equations:

$$\dot{\mathbf{x}} = \mathbf{f}(\mathbf{x}; \mu) \tag{1}$$

in which $\mathbf{x}(t) \in \mathbb{R}^n$ is a vector valued function depending on a parameter t called the time and $\mathbf{f}$, the so-called vector field, is a n-component smooth function generating a flow ϕ_t. $\mu \in \mathbb{R}^p$ is the parameter vector with p components, assumed to be constant in this paper. The system (1) is called the original system (OS). As stated in the introduction the systems studied are such that $n = 3$. The OS may therefore be written as:

$$\begin{cases} \dot{x} = f_1(x, y, z) \\ \dot{y} = f_2(x, y, z) \\ \dot{z} = f_3(x, y, z) \end{cases} \tag{2}$$

It is then assumed that the observer numerically records a scalar time signal. By convention in this section, the observable is taken to be $x_1 = x$.

The aim is to reconstruct a vector field equivalent (we will see in which sense) to the OS under the form of a standard system (SS) made of the observable and of its derivatives according to:

$$\begin{cases} \dot{X} = \dot{x} = Y \\ \dot{Y} = Z \\ \dot{Z} = F(X, Y, Z) \end{cases} \tag{3}$$

in which the standard state space related to SS is spanned by standard coordinates (X, Y, Z) with $X = x$ and in which F is called the standard function. In this paper, we only consider the case when the SS has a dimension m equal to 3. A so-called standard transformation Φ expressing the standard coordinates $\{X, Y, Z\}$ *versus* the original coordinates $\{x, y, z\}$ may then be obtained according to:

$$\Phi \equiv \begin{cases} X = x \\ Y = f_1(x, y, z) \\ Z = \dfrac{\partial f_1}{\partial x} f_1 + \dfrac{\partial f_1}{\partial y} f_2 + \dfrac{\partial f_1}{\partial z} f_3 \end{cases} \tag{4}$$

Therefore, Φ: $\mathbb{R}^n \to \mathbb{R}^m$ is a well-defined transformation without any singularity since the original vector field $\mathbf{f}$ is smooth. Let us now focus on the attractor A_{OS} defined by $(x(t), y(t), z(t))$ in the limit $t \to \infty$. The attractor A_{SS} of the SS may be obtained from A_{OS} by using Φ. Also, as the OS is known, algebraic manipulations allow us to find the standard function $F(X, Y, Z)$.

We are now interested to know how A_{OS} is mapped by Φ and the nature of the equivalence between A_{OS} and A_{SS}. Algebraic considerations on Φ determine whether the transformation is an embedding, an immersion or worst an immersion that fails to be one-to-one [21].

When Φ defines a diffeomorphism, the reconstructed attractor is subject to the most restrictive requirements possible. Such a diffeomorphic equivalence between original and reconstructed attractors may be proved on the local properties of the transformation Φ. When $m = n$, this is achieved following the inverse function theorem [22, 23] leading to the result that the transformation Φ is a diffeomorphism if its Jacobian matrix $D\Phi$ is nowhere singular. Such a diffeomorphism may be found between the original Rössler attractor [24] and the attractor reconstructed from its y-variable while x- and z-variables provide transformations Φ_x and Φ_z whose Jacobian matrix vanishes on a set of Lebesgue measure zero. These facts may readily be checked by the reader with a small amount of algebra. Φ_x and Φ_z define therefore almost everywhere a diffeomorphism. Consequently, the y-variable is the best observable to reconstruct the dynamics of the Rössler system from a time scalar series.

It must be noted, however, that the transformation Φ could be considered as an embedding even though it fails to pass the analytical test in some subsets of the original phase space. Indeed, we are only interested in the properties of the restriction of the map to the strange attractor, which is a subset of volume zero. Presumably, singularities located outside of the strange attractor should not matter as long as a global vector field reconstruction is not the issue considered.

Nevertheless, we are here essentially concerned by statements about the possibility of preserving the topological properties of A_{OS} through Φ and this aim must be reached by achieving a topological characterization of the attractors. Then, as the original system is assumed to be known in this paper (although it is usually not known when we deal with experimental

systems), an attractor may be reconstructed from each variable by applying a corresponding Φ to the original time vector series. For a given system, we call A_{OS} the attractors which are spanned by the original coordinates (x, y, z). The reconstructed attractor which is spanned by derivative coordinates (X, Y, Z) will be noted by A_x, A_y and A_z where the subscript is associated with the observable used. Transformations Φ_x, Φ_y and Φ_z which map the original coordinates (x, y, z) to the derivative coordinates (X, Y, Z) may be easily obtained by using equation (4), in which the subscript is again associated with the observable used. In any case, X will be associated with the scalar time series from which the attractor is reconstructed.

2.2. TOPOLOGICAL CHARACTERIZATION. — Over the past few years several studies have discussed the topological description of chaotic attractors. In particular the idea has arisen that an attractor can be described by the population of periodic orbits, their related symbolic dynamics and their linking numbers [25]. In three-dimensional cases, periodic orbits may be viewed as knots [31] and, consequently, they are robust with respect to smooth parameter changes and allow the definition of topological invariants under isotopy.

The topological approach is based on the organization of periodic orbits. Since periodic orbits are dense in hyperbolic strange attractors, knowledge of their linking properties severely constrains the topology of the strange attractor. As recently advocated [26–28], the quantitative topological characterization of low dimensional chaotic sets could proceed in a few steps. First, the strange set is assigned a good symbolic encoding. In the case of very dissipative systems, it is possible to model the first-return map — which maps the Poincaré surface into itself — using a map of an interval into itself. A natural encoding is then given with respect to the critical points of the first-return map. It is a good symbolic encoding which assigns different symbolic sequences to different periodic orbits. For more convenience, we label monotonic branches of the first-return map by integers whose parity is related to the parity of the local torsion (expressed in term of π) of the corresponding strip on the template, *i.e.* an even (odd) label of a branch corresponds to a strip having an even (odd) number of local torsions. The population of unstable periodic orbits is then extracted by a close return method [29] and encoded.

We have to mention that we characterize periodic orbits not only by linking numbers but also by topological periods associated with the Poincaré section. Indeed, topological analysis involves comparing the periodic orbits in phase space with projections on the surface of a template. Two links which cannot be distinguished by invariants of ambient isotopy (*e.g.* linking numbers) but involve orbits having different topological periods cannot be considered as being identical. While any regular plane projection may be used to determine linking numbers, the topological period of an orbit strongly depends on the choice of a Poincaré surface, since it is given by the number of intersections of the orbit with this surface.

A Poincaré surface must be transverse to the flow. The direction in which the Poincaré surface is traversed by the trajectory has also to be considered. Generically, this direction changes at a fixed point around which trajectories are developed. Consequently, a Poincaré surface may be conveniently chosen as containing a fixed point. Unfortunately, there are no more detailed prescriptions to define a good Poincaré surface which may crucially depend on the system studied.

In the next stage, ribbon subsets, here called bands, are identified in a 3D representation, *i.e.* the local torsion $L(i, i)$ of each band is determined and the linking numbers $L(i, j)$ of the ribbon graph for the i^{th} and j^{th} bands is extracted. A linking matrix with diagonal matrix elements $L(i, i)$ and off-diagonal matrix elements $L(i, j) = L(j, i)$ is proposed. The off-diagonal elements are equal to the sum of the crossings between the i^{th} and j^{th} bands of the ribbon graph with a standard insertion [30].

The template is then checked by extracting the linking number $L(N_1, N_2)$ of a pair of orbits N_1 and N_2 in a plane projection. For this operation one only needs to count the signed crossings of a pair of orbits N_1 and N_2 in a *regular plane projection* of the pair (a drawing of it such that no more than two lines cross at any point). After assigning an orientation to the periodic orbits with respect to the flow and defining a number $\epsilon_{12}(p) = \pm 1$ for *right/left*-handed crossings p between N_1 and N_2 [30], the linking number is given by:

$$L(N_1, N_2) = \frac{1}{2} \sum_p \epsilon_{12}(p) \tag{5}$$

which is a topological invariant. Then, orbits N_1 and N_2 are constructed on the template (the procedure is reported in detail in [31]). Finally, linking numbers are compared: the template is validated if the linking number obtained from the regular plane projection is equal to the one obtained from the corresponding orbits constructed on the template.

As the template which carries the periodic orbits is identified, the organization of the orbits is known. For a complete discussion of the equivalence between periodic orbits embedded within a strange attractor and orbits of the template, see [32].

3. Is A_{SS} Equivalent to A_{OS}?

The system studied in this paper is generated by three equations, *i.e.* there are three original coordinates, namely (x, y, z). Each of these coordinates may be taken as the observable and, consequently, three different cases may be investigated for each system. Only the most interesting results will be discussed.

Although only one variable of the Rössler system provides a reconstructed attractor diffeomorphically equivalent to the original Rössler attractor, attractors reconstructed from the other variables (x and z) are topologically equivalent to the original one by using delay coordinates [32] as well as derivative coordinates [33]. By topologically equivalent, we mean that any two periodic orbits in the reconstructed phase space have the same topological invariants as the corresponding orbits in the original phase space. But the Rössler system is a very simple folded band and it is definitely worth studying more complicated cases. For instance, let us examine the case of the well-known Lorenz system which exhibits symmetry properties.

3.1. Original Phase Space. — In the case of the Lorenz system, the problem becomes a little more tricky. Two kinds of configuration related to the equivariance properties of the system appear. (i) x- and y-observables are equivariant and provide attractors A_x and A_y with symmetry properties, respectively (Figs. 1a and b), (ii) z-observable is invariant and provides an attractor A_z without any symmetry (Fig. 1c). It is clear that all the information on symmetry is lost in A_z. King and Stewart [34] showed that the use of an equivariant observable is required to guarantee a reconstructed attractor with symmetry properties. Unfortunately, even now, we are not sure that the symmetry properties are identical to the original ones, as illustrated below.

In the whole space, the Lorenz system reads as:

$$\begin{cases} \dot{x} = \sigma(y - x) \\ \dot{y} = Rx - y - xz \\ \dot{z} = -bz + xy \end{cases} \tag{6}$$

in which we use a control parameter vector $(R, \sigma, b) = (28, 10, 8/3)$ for which the asymptotic motion settles down onto a strange chaotic attractor [19].

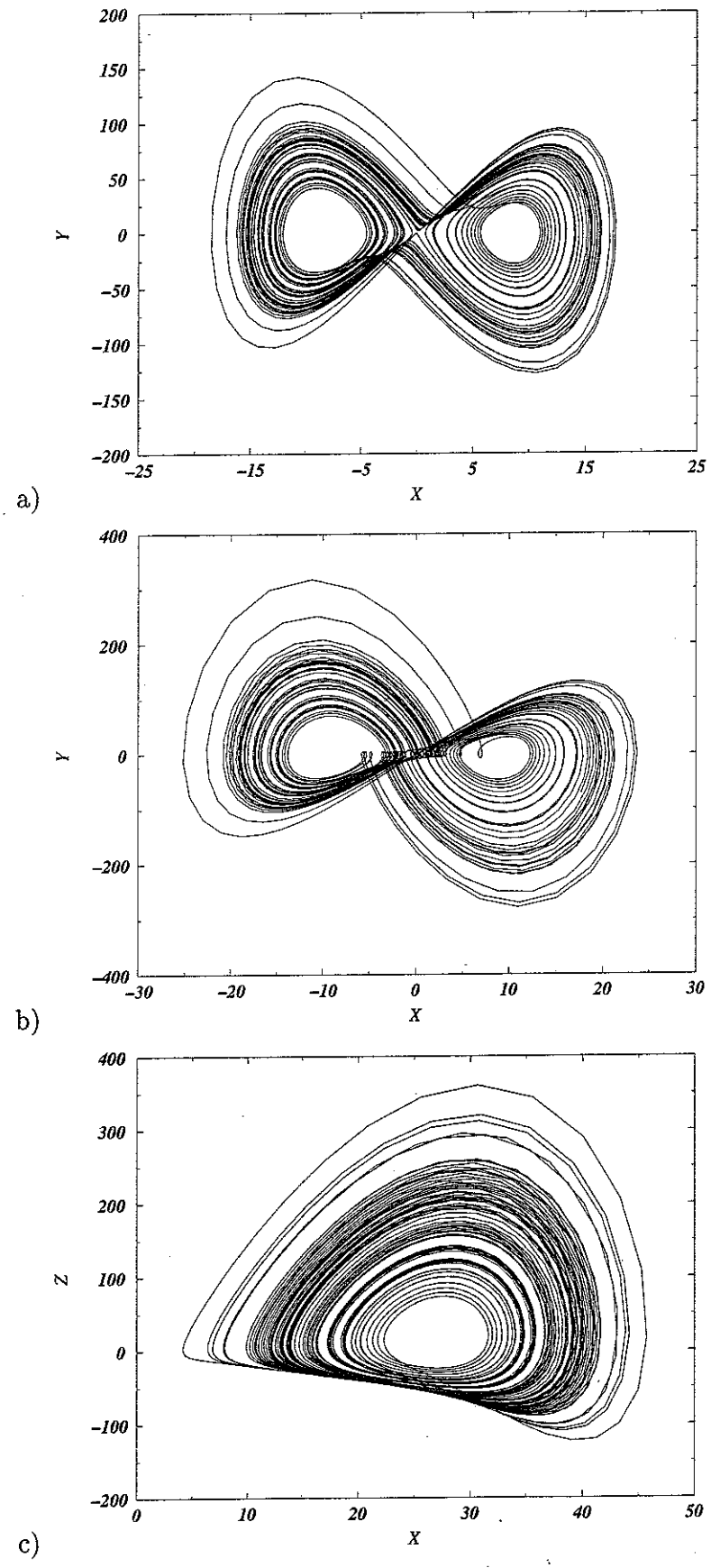

Fig. 1. — Attractors reconstructed from different variables of the Lorenz system: a) Attractor A_x, b) Attractor A_y, c) Attractor A_z.

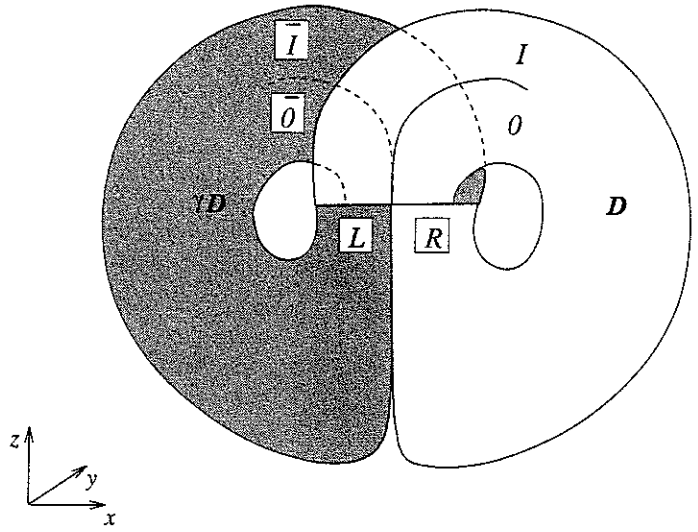

Fig. 2. — Schematic view of the fundamental domain $\mathcal{D}$ as the right wing and its copy $\gamma\mathcal{D}$ as the left wing.

The system has three fixed points reading as:

$$F_0 = \begin{vmatrix} 0 \\ 0 \\ 0 \end{vmatrix}, \qquad F_+ = \begin{vmatrix} x_+ \\ y_+ \\ z_+ \end{vmatrix} \quad \text{and} \quad F_- = \begin{vmatrix} x_- \\ y_- \\ z_- \end{vmatrix}$$

where $x_\pm = y_\pm = \pm\sqrt{b(R-1)}$ and $z_\pm = R - 1$.

One may note that the vector field $\mathbf{f}$ defined by equation (6) is equivariant, *i.e.*

$$\mathbf{f}(\gamma\mathbf{x}, \mu) = \gamma\mathbf{f}(\mathbf{x}, \mu) \tag{7}$$

where γ is a matrix defining the equivariance. In the Lorenz case, the matrix γ is given by:

$$\gamma = \begin{pmatrix} -1 & 0 & 0 \\ 0 & -1 & 0 \\ 0 & 0 & 1 \end{pmatrix} \tag{8}$$

In other words, the original Lorenz attractor A_{OS} is invariant under the action of γ which defines an axial symmetry.

This symmetry induces specific considerations such as defining a fundamental domain $\mathcal{D}$ which tasselates the complete state space [35, 36]. Indeed, as the Lorenz dynamics is invariant under the action of γ, the state space can be tiled by a fundamental domain $\mathcal{D}$ and one of its copy $\gamma\mathcal{D}$ (note that $\gamma^2\mathcal{D} = \mathcal{D}$). In the Lorenz attractor, the fundamental domain may be viewed as a wing: in Figure 2 the fundamental domain $\mathcal{D}$ is displayed as the right wing and its copy $\gamma\mathcal{D}$ as the left wing. More precisely, the fundamental domain $\mathcal{D}$ is separated from its copy by the invariant surface $\mathcal{S}$ under the action of γ, *i.e.*

$$\mathcal{S} \equiv \left\{(x, y, z) \in \mathbb{R}^3 \mid y = -x\right\} \tag{9}$$

Consequently, the fundamental domain may be defined as

$$\mathcal{D} \equiv \left\{(x, y, z) \in \mathbb{R}^3 \mid y > -x\right\} \tag{10}$$

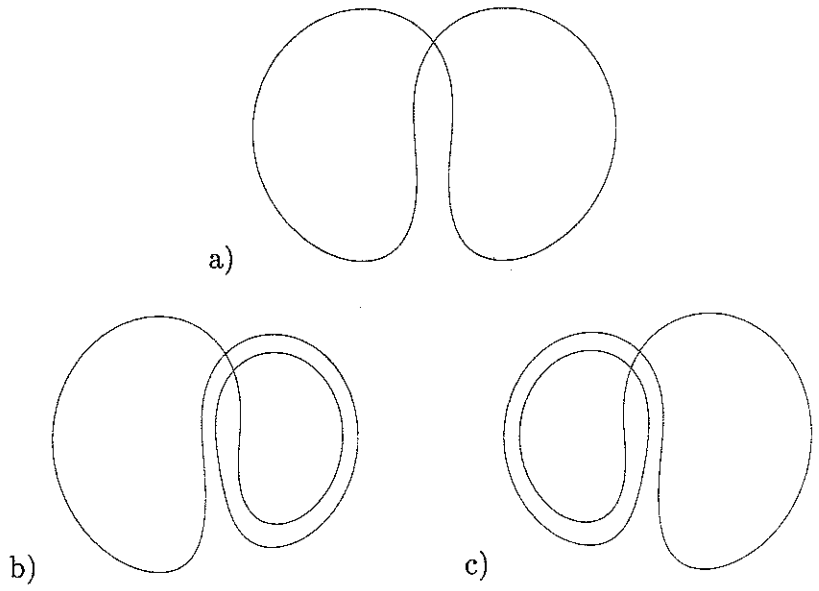

Fig. 3. — Symmetric orbit a) and a pair of asymmetric orbits b) and c). a) Symmetric orbit encoded (RL), b) asymmetric orbit encoded (LRR), c) asymmetric orbit encoded (RLL).

while its copy is defined as

$$\gamma\mathcal{D} \equiv \left\{(x, y, z) \in \mathbb{R}^3 \mid y < -x\right\} \tag{11}$$

It must be noted that the choice of $\mathcal{D}$ and $\gamma\mathcal{D}$ is quite arbitrary and, consequently, $\mathcal{D}$ and $\gamma\mathcal{D}$ could be inverted.

For the sake of clarity, we must introduce a symbolic dynamics working in the whole phase space before carrying out the topological analysis. Such symbolic dynamics was first introduced by Birman and Williams [37] as displayed in Figure 2. All periodic orbits may thus be encoded in the obvious way with symbols on the set $\{\mathrm{L}, \mathrm{R}\}$ following the trajectory. In this case, a symbol is associated with each revolution of the trajectory around one of the fixed points F_+ or F_-. The topological period of an orbit is thus clearly related to the number of revolutions around F_+ and F_-. The population of periodic orbits is reported in Table I.

Two kinds of periodic orbits may then be distinguished. First, we have symmetric orbits (Fig. 3a) which are globally invariant under the action of γ. Their symbolic sequence may be written under the form (WW*) where W* is the conjugate of W, *i.e.* R is mapped to L and *vice versa*. The period of such an orbit is therefore even. Next, we have asymmetric orbits (Figs. 3b and c) which are mapped to each other under the action of γ to their symmetric configuration and therefore appear in pairs. For instance, the orbit encoded by (LRR) (Fig. 3b) is mapped to the orbit encoded by (RLL) (Fig. 3c) under the action of γ. Their symbolic sequences are conjugate.

This symbolic dynamics has been successfully used by many authors as exemplified by Sparrow [38]. Such symbolic dynamics is not compatible with the existence of a two strip template [39]. This is because it is impossible to build a template with two strips playing a symmetric role. A four strip template may, however, successfully predict the linking numbers counted in a regular plane projection of periodic orbits. Such a template is displayed in Figure 4. Consequently, symbolic dynamics on the set $\{\overline{0}, \overline{1}, 1, 0\}$ is required to encode periodic orbits on this template. Note that symbols $\overline{0}$ and $\overline{1}$ are the conjugate of 0 and 1, respectively. The necessity of using 4 symbols for the template and only 2 (L and R) to encode the orbits is

Table I. — *Population of periodic orbits within the Lorenz attractor for $R = 28$: $y = (b(R - 1))^{1/2}$. For each periodic orbit, the symbolic sequences in the whole phase space and in the fundamental domain $\mathcal{D}$ are given.*

in the whole space		in $\mathcal{D}$	
	RL		1
	RLLR		10
LRR		RLL	101
	RLLLRR		100
	RLLRLRRL		1011
LRRR		RLLL	1001
	RLLLLRRR		1000
LRRLR		RLLRL	10111
	RLLRLLRRLR		10110
LRRLL		RLLRR	10010
	RLLLRLRRRL		10011
LRRRR		RLLLL	10001
	RLLLLLRRRR		10000
LRRLRL		RLLRLR	101110
	RLLRLRLRRLRL		101111
	RLLLRRLRRRLL		100101
LRRRLR		RLLLRL	100111
	RLLLRLLRRRLR		100110
LRRRRL		RLLLLR	100010
	RLLLLRLRRRRL		100011
LRRRRR		RLLLLL	100001
	RLLLLLLRRRRR		100000
LRRLRLR		RLLRLRL	1011111
	RLLRLRLLRRLRLR		1011110
LRRLRRL		RLLRLLR	1011010
	RLLRLLRLRRLRRL		1011011
LRRRLLR		RLLLRRL	1001011
	RLLLRRLLRRRLLR		1001010
LRRRLRL		RLLLRLR	1001110
	RLLLRLRLRRRLRL		1001111
LRRRLRR		RLLLRLL	1001101
	RLLLRLLLRRRLRR		1001100
LRRRRLL		RLLLLRR	1000100
	RLLLLRRLRRRRLL		1000101
LRRRRLR		RLLLLRL	1000111
	RLLLLRLLRRRRLR		1000110
LRRRRRL		RLLLLLR	1000010
	RLLLLLRLRRRRRL		1000011
LRRRRRR		RLLLLLL	1000001
	RLLLLLLLRRRRRR		1000000

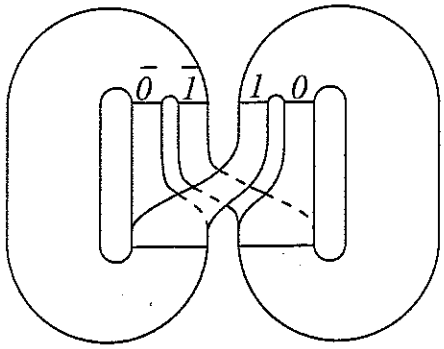

Fig. 4. — Four strip template obtained by dividing each wing in two strips: one, labelled by 0 or $\bar{0}$, associated with the reinjection of the trajectory in the same wing, and one, labelled by 1 or $\bar{1}$, associated with the transition from one wing to the other.

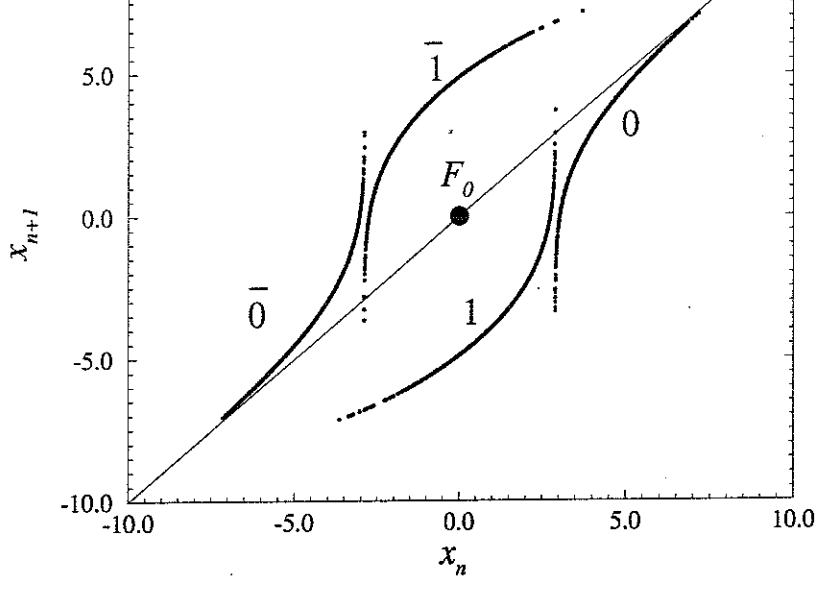

Fig. 5. — First-return map to the Poincaré section P_w computed with the x-variable. Each monotonic branch is associated with a strip of the template according to the symbols on the set $\{\bar{0}, \bar{1}, 1, 0\}$.

a shortcoming which will be canceled by accounting for the symmetry, *i.e.* by projecting the dynamics on fundamental domains.

This discussion may also be illustrated by computing a first-return map in a Poincaré section P_w reading as:

$$P_w \equiv \left\{(x, y) \in \mathbb{R}^2 \mid z = R - 1\right\} \tag{12}$$

The x-variable is then used to compute the first-return map which is made up of four monotonic branches exhibiting an inversion symmetry relative to the fixed point F_0 (Fig. 5).

Symbols of the set $\{\bar{0}, \bar{1}, 1, 0\}$ act as transition symbols. Thus, for instance, two revolutions on the left wing corresponding to a sequence (LL), *i.e.* without any transition is mapped to $\bar{0}$, and a sequence (LR), exhibiting a transition from the left to the right wing, is mapped to $\bar{1}$ (see Fig. 3). Therefore blocks of two letters in the code $\{R, L\}$ are mapped to one letter in

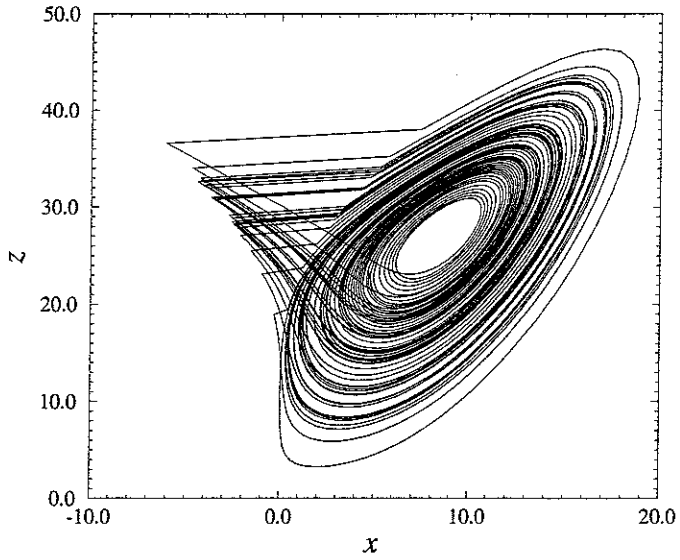

Fig. 6. — Dynamics of the Lorenz system projected on the fundamental domain $\mathcal{D}$.

the code $\{\overline{0}, \overline{1}, 1, 0\}$. As a whole, we may define a mapping Ψ sending blocks of two letters in $\{\mathrm{R}, \mathrm{L}\}$ to one letter in $\{\overline{0}, \overline{1}, 1, 0\}$, reading as:

$$\Psi \equiv \begin{cases} \Psi(\mathrm{LL}) = \overline{0} \\ \Psi(\mathrm{LR}) = \overline{1} \\ \Psi(\mathrm{RL}) = 1 \\ \Psi(\mathrm{RR}) = 0 \end{cases} \tag{13}$$

For instance, the orbit $(\mathrm{LRR}) = \mathrm{LRRLRR}...$ is mapped to $\overline{1}01\overline{1}01... = (\overline{1}01)$.

3.2. In the Fundamental Domain. — It has been shown that the dynamical analysis of such a system may be more conveniently achieved by working in the fundamental domain in which all the trajectory is projected [35, 36]. Indeed, taking into account the equivariance property, the dynamical behaviour on the fundamental domain is the same as on its copy. Consequently, knowing the topological organization in the fundamental domain and the nature of the equivariance provides all the required topological information on the whole attractor. The template associated with the fundamental domain is then much simpler than on the whole attractor and is therefore given a due privilege. Furthermore, restricted topological equivalence allows us to compare the topological organization of different attractors tasselated by different numbers of fundamental domains, *i.e.* different symmetry orders. Therefore the comparison between the spectra of periodic orbits, from the point of view of the symbolic dynamics, is allowed.

In order to achieve a topological characterization of the fundamental domain, all the dynamics has first to be projected on the fundamental domain as displayed in Figure 6. A given periodic orbit in the whole space reading as:

$$\xi \equiv \{\mathbf{X}_\xi(t)\}_{t=0}^{T_\xi} \tag{14}$$

where $\mathbf{X}_\xi(t)$ is the coordinate vector at time t of the periodic orbit ξ, and T_ξ is its time period,

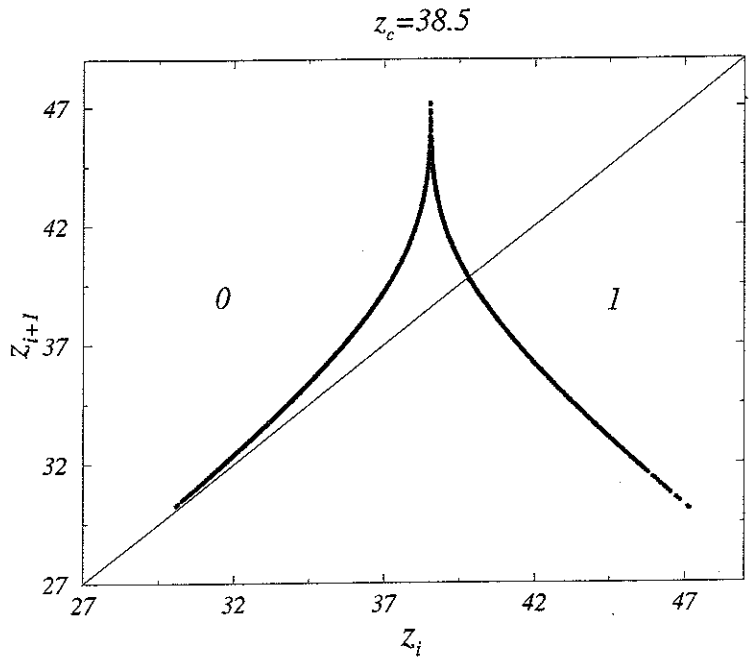

Fig. 7. — First-return map on the Poincaré set $P_{\mathcal{D}}$ built with the invariant z-variable.

is then projected on the fundamental domain to a fundamental periodic orbit reading as:

$$\xi_{\mathcal{D}} \equiv \{\mathbf{Y}_\xi(t) \mid \mathbf{Y}_\xi(t) = \gamma \mathbf{X}_\xi(t) \text{ if } y < -x \quad , \quad \mathbf{Y}_\xi(t) = \mathbf{X}_\xi(t) \text{ otherwise } \}_{t=0}^{T_\xi} \tag{15}$$

A Poincaré section $P_{\mathcal{D}}$ of the fundamental domain $\mathcal{D}$ is then defined as

$$P_{\mathcal{D}} \equiv \left\{ (x,z) \in \mathbb{R}^2 \mid y = y_+, \ \frac{\partial \mathbf{f}_z}{\partial y} < 0 \right\} \tag{16}$$

where $\mathbf{f}$ is the vector field defined in equation (6). The first-return map is displayed in Figure 7 and is found to be similar to the well-known Lorenz map [19]. This is due to the fact that the Lorenz map is computed with the z-invariant variable which does not distinguish the fundamental domain $\mathcal{D}$ from its copy $\gamma\mathcal{D}$.

This first-return map allows us to encode periodic orbits as follows:

$$K(z) = \begin{cases} 0 & \text{if} \quad z < z_c \\ 1 & \text{if} \quad z > z_c \end{cases} \tag{17}$$

where $K(z)$ is the code of the z-coordinate of the trajectory in the Poincaré set $P_{\mathcal{D}}$. The population of fundamental periodic orbits is reported in Table I.

In order to define the linking properties of fundamental periodic orbits, we introduce the fundamental linking numbers $\mathcal{L}(N_i, N_j)$ which are counted on the fundamental domain and defined as:

$$\mathcal{L}(N_i, N_j) = \frac{1}{2} \sum_p \epsilon_{ij}(p) \qquad (i \neq j) \tag{18}$$

where ϵ_{ij} designates oriented crossings between two fundamental orbits. Fundamental linking numbers $\mathcal{L}(N_i, N_j)$ have to be equal to the linking numbers predicted by the template which synthesizes the topology of the fundamental domain. Such a template may be called a fundamental template in contrast with the more complex template which is associated with the

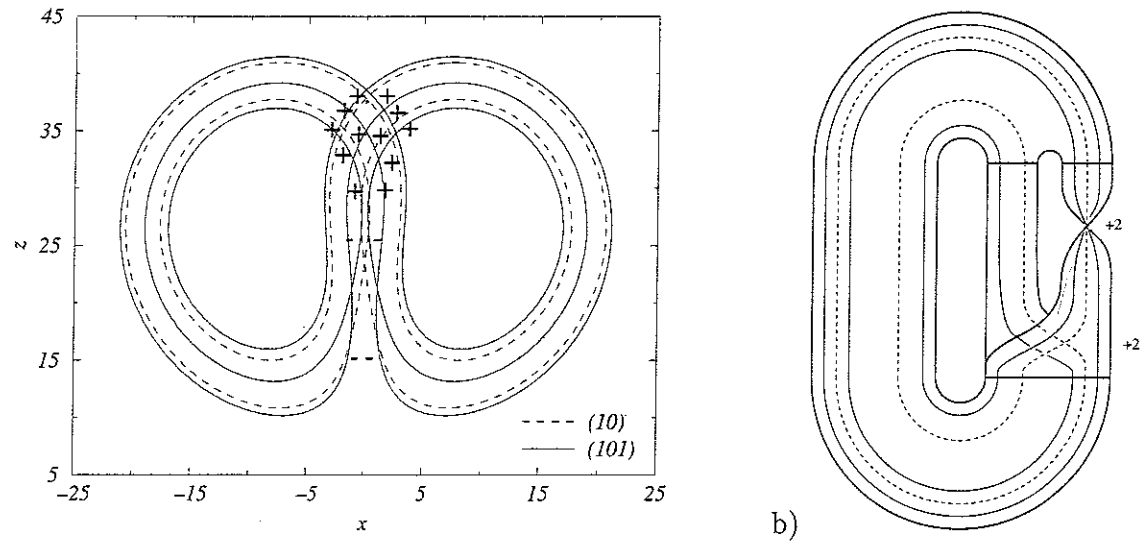

Fig. 8. — Checking of the fundamental linking number $\mathcal{L}(101, 10)$ between the plane projection and the template construction of orbit pair (101, 10). a) $\mathcal{L}(101, 10) = \frac{1}{2}(+4) = +2$, b) $\mathcal{L}(101, 10) = \frac{1}{2}(+4) = +2$

Table II. — *Fundamental linking numbers between pairs of orbits whose period is less than 5.*

	(1)	(10)	(101)	(100)	(1011)	(1001)
(10)	+1					
(101)	+1	+2				
(100)	+1	+2	+3			
(1011)	+2	+3	+4	+4		
(1001)	+1	+2	+3	+3	+4	
(1000)	+1	+2	+3	+3	+4	+4

whole attractor. As an example, the fundamental linking number $\mathcal{L}(101, 10)$ is counted on a plane projection of the fundamental orbits encoded by (101) and (10) (see Fig. 8).

In the same manner, we determine linking numbers between all pairs of orbits whose period is less than 5. These linking numbers are reported in Table II. All these linking numbers are found to be well predicted by the template described by the linking matrix M_{ij} reading as:

$$M_{ij} = \begin{pmatrix} 0 & 0 \\ 0 & +1 \end{pmatrix} \tag{19}$$

This template is displayed in Figure 8b where a construction of the pair (101, 10) is given as an example allowing the fundamental linking number $\mathcal{L}(101, 10)$ to be checked. The template obtained is furthermore found to be in agreement with the Lorenz map, *i.e.* a band 0 (even local torsion) is associated with the increasing (orientation preserving) branch of the map and a band 1 (odd local torsion) is associated with the decreasing (orientation reversing) branch of the map. A similar template is obtained from $\gamma\mathcal{D}$.

3.3. Attractor Induced by an Equivariant Variable. — Let us consider the attractor reconstructed from an equivariant variable that we may obtain by integrating a reconstructed vector field or by using derivative coordinates. The same reconstructed attractor may also be

obtained by applying a standard transformation Φ (Eq. (4)) to the original attractor. The reconstruction technique relies on the analysis of a scalar time series. When the observable used is equivariant, then the reconstructed attractor is governed by equivariant variables only because the derivatives of equivariant variables are equivariant too. Consequently, the reconstructed system is unchanged under the action of a γ-matrix which reads as:

$$\gamma = \begin{pmatrix} -1 & 0 & 0 \\ 0 & -1 & 0 \\ 0 & 0 & -1 \end{pmatrix} \tag{20}$$

and defines an inversion symmetry which is not necessarily present in the original vector field. Indeed, the original Lorenz vector field is composed of two equivariant and an invariant variables. Consequently, a system whose original equivariance defines an axial symmetry is reconstructed as a system whose equivariance defines an inversion symmetry when an equivariant variable is used. As stated by King and Stewart [34], techniques for phase space reconstruction from an equivariant scalar time series are failing to obtain attractors whose symmetry is identical to the original symmetry. As an example taken here, the Lorenz system exhibiting an axial symmetry (see equivariance matrix of Eq. (8)) is mapped to a reconstructed system which possesses the equivariance matrix of equation (20), when the observable is equivariant. Of course, this equivariance is not directly related to the Lorenz system. It is therefore rather interesting to discuss the restricted topological equivalence between such a reconstructed attractor and the original one. In order to do that, we have to extract the fundamental template of the reconstructed attractor A_x generated by the equivariant variable x, taken as an example. In this case, the reconstructed space is spanned by $(X, Y, Z) = (x(t), \dot{x}(t), \ddot{x}(t))$.

The fundamental domain cannot obviously be defined in terms of an invariant surface since only a single point, namely the origin of the reconstructed space, is invariant under the action of the γ-matrix. Nevertheless, we may practically define the fundamental domain as defined by

$$\mathcal{D} \equiv \left\{(X, Y, Z) \in \mathbb{R}^3 \mid X < 0\right\} \tag{21}$$

and its copy

$$\gamma\mathcal{D} \equiv \left\{(X, Y, Z) \in \mathbb{R}^3 \mid X > 0\right\} \tag{22}$$

where $X = 0$ is here considered as an invariant surface. Once the dynamics is projected on the fundamental domain, we compute a first-return map into a Poincaré section $P_{\mathcal{D}_x}$ defined as:

$$P_{\mathcal{D}_x} \equiv \left\{(Y, Z) \in \mathbb{R}^2 \mid X = X_F,\ \dot{X} < 0\right\} \tag{23}$$

where $X_F = \sqrt{b(R-1)}$. The first-return map can then be independently computed from the Y- or Z-variables. An equivalent first-return map may be obtained by using a Poincaré set P_X in the whole space which is defined as $P_X = P_{X_+} \cup P_{X_-}$ where:

$$P_{X_+} = \left\{(Y, Z) \in \mathbb{R}^2 \mid X = X_F, \dot{X} < 0\right\} \tag{24}$$

and

$$P_{X_-} = \left\{(Y, Z) \in \mathbb{R}^2 \mid X = -X_F, \dot{X} > 0\right\} \tag{25}$$

To mod out the symmetry, the map is hereafter computed with an invariant variable which may be the natural invariant Z-variable or the less natural but efficient $|Y|$-variable. A map similar to the Lorenz map is obtained in which the critical point is located at $|Y_c| = 78$ (Fig. 9).

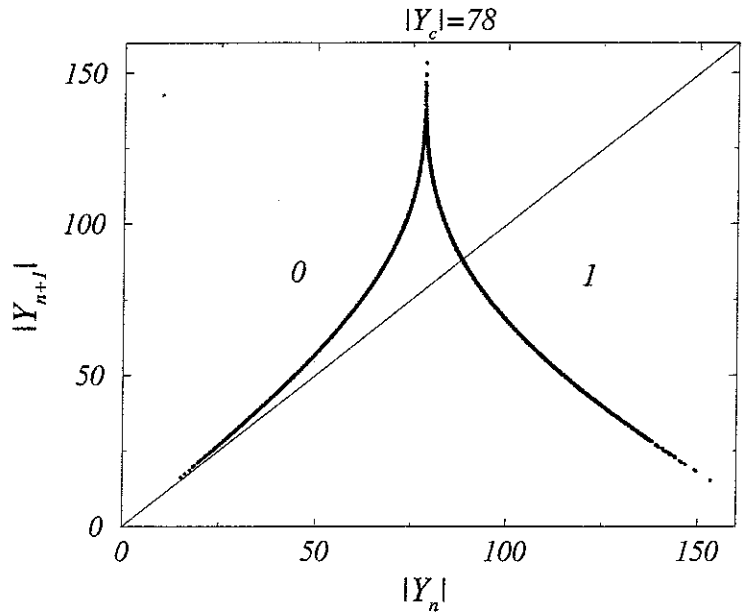

Fig. 9. — First-return map to the Poincaré set P_X of the A_x.

As on the original attractor, the increasing branch, labelled 0, is associated with the reinjection of the trajectory in the same wing and the decreasing branch, labelled 1, with the transition from one wing to the other.

Nevertheless, there exists a deep difference between the original attractor and the reconstructed attractor A_x since the symmetry properties are different. Indeed, the fundamental template induced by the original attractor was found to be independent of the choice of the fundamental domain, *i.e.* $\mathcal{D}$ and $\gamma\mathcal{D}$ induce the same template. Conversely, in the reconstructed attractor, the strip of $\mathcal{D}$ associated with the increasing branch of the first-return map undergoes a positive π-twist while the strip of $\gamma\mathcal{D}$ associated with the same branch of the map undergoes a negative π-twist (Fig. 10a).

In the previous section, we have presented the topological procedure to characterize an attractor in a case where the symmetry preserves the local torsion sign but this condition is not met in the case of an inversion symmetry. In fact an inversion symmetry reverses the local torsion sign (Fig. 11). This property will have deep consequences on the fundamental linking numbers $\mathcal{L}(N_i, N_j)$ as described below.

From the mask of A_x (Fig. 10a), we extract the masks associated with the fundamental domain $\mathcal{D}$ and its copy $\gamma\mathcal{D}$, respectively (Fig. 10b). Let us insist on the fact that Figure 10b presents both $\mathcal{D}$ and $\gamma\mathcal{D}$, *i.e.* exhibits two fundamental domains in so far as either $\mathcal{D}$ or $\gamma\mathcal{D}$ could be chosen as the fundamental domain, this choice being arbitrary. Two fundamental templates are then proposed (Fig. 10c). Note that the fundamental template associated with the fundamental domain $\mathcal{D}$ presents a band 1 with a positive π-twist and the template associated with its copy $\gamma\mathcal{D}$ has a band 1 with negative π-twist: this is a consequence of the inversion symmetry which reverses the local torsion sign in contrast with the previously discussed case of axial symmetry. Then, using the standard insertion convention, the templates are described by the linking matrices

$$M_{\mathcal{D}} = \begin{pmatrix} 0 & 0 \\ 0 & +1 \end{pmatrix} \quad \text{and} \quad M_{\gamma\mathcal{D}} = \begin{pmatrix} 0 & -1 \\ -1 & -1 \end{pmatrix}, \tag{26}$$

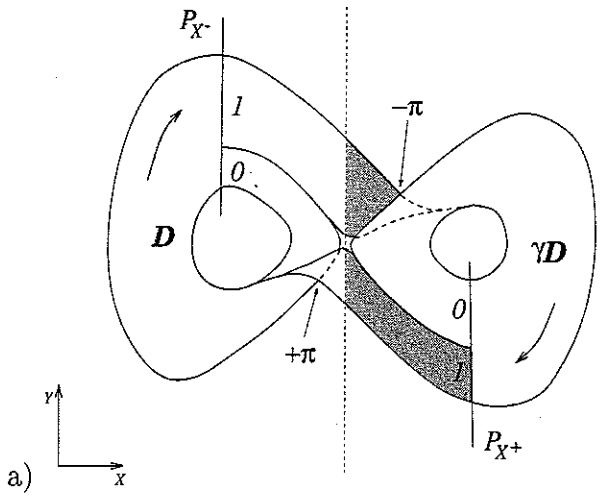

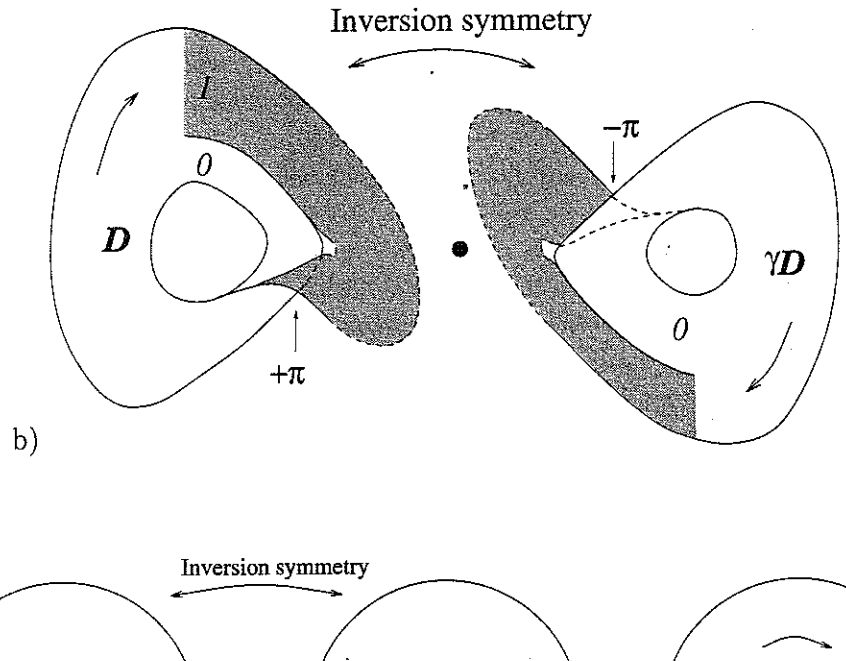

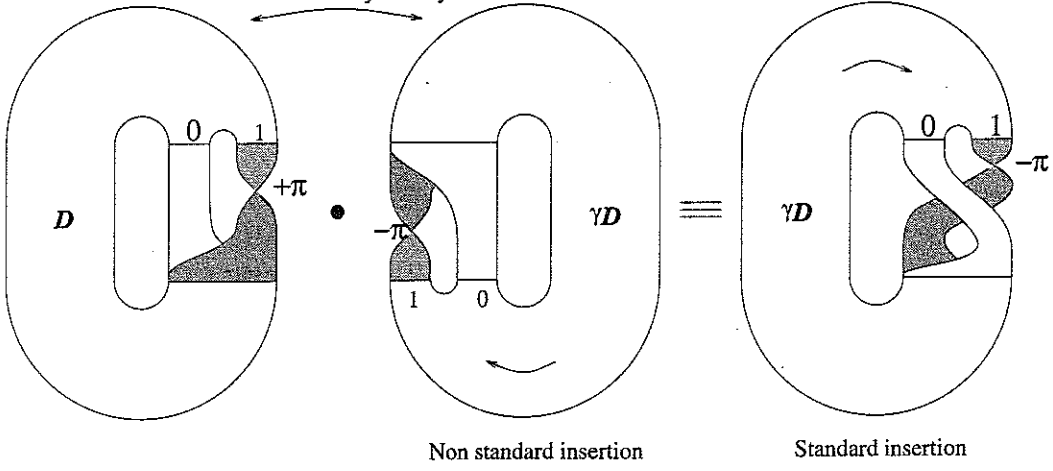

Fig. 10. — Extraction of the x-induced template. a) Equivariant mask of A_x: the fundamental domain $\mathcal{D}$ and its copy $\gamma\mathcal{D}$ are bounded by the dashed line. The Poincaré sections P_{X_+} and P_{X_-} are also displayed. b) Schematic views of the masks associated with $\mathcal{D}$ and $\gamma\mathcal{D}$ of A_x. c) Templates of the fundamental domain $\mathcal{D}$ and its copy $\gamma\mathcal{D}$.

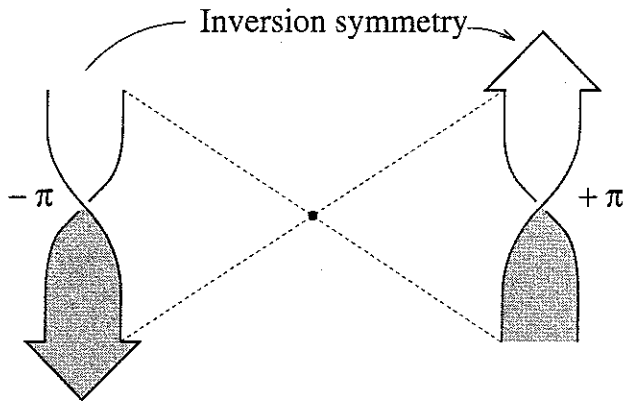

Fig. 11. — Local torsion sign is reversed under a inversion symmetry.

respectively. Note that the template of the fundamental domain is the same as for the fundamental domain of the original attractor. Consequently, if we mod out the symmetry, the template of the reconstructed attractor induced by the x-time series is the same as the original Lorenz system. So the two different dynamical systems have a fundamental domain exhibiting the same structure (horseshoe dynamics).

As both fundamental templates topologically characterize the attractor (in the restricted sense), we cannot determine the sign of the local torsion of band 1. Consequently, as the choice of the fundamental domain $\mathcal{D}$ is arbitrary (the right wing could be also chosen as the fundamental domain), the sign of the fundamental linking number $\mathcal{L}(N_i, N_j)$ is arbitrary too. For these reasons, we prefer to introduce an unsigned fundamental linking number $\tilde{\mathcal{L}}(N_i, N_j)$. Let us note that the introduction of unsigned fundamental linking numbers is deeply related to the fact that restricted topological equivalence is not topological equivalence in the strict sense (indeed topological equivalence requires the use of signed linking numbers).

We now emphasize the usefulness of working with such a fundamental domain (at least in the present case of inversion symmetry). Due to the inversion symmetry which reverses the local torsion sign, a signed crossing on a wing of A_x is opposite to its corresponding crossing (under the action of γ) on the other wing. Thus the linking numbers $L(N_i, N_j)$ between two symmetric orbits are always equal to 0. So topological equivalence in the strict sense does not discriminate sufficiently between different dynamics associated with symmetrical orbits. Topological characterization should therefore preferably be performed by considering a fundamental domain and a fundamental linking number.

Thus, as signed crossings are reversed under the action of γ, fundamental linking numbers are found to be positive in the fundamental domain $\mathcal{D}$ and negative in its copy. Indeed, one may check that the fundamental linking number $\mathcal{L}(101, 10)$ is found to be equal to $+2$ in the fundamental domain while it is found to be equal to -2 in its copy $\gamma\mathcal{D}$ (Fig. 12). One may check in Figure 12 that each oriented crossing of $\mathcal{D}$ is mapped to an opposite crossing on $\gamma\mathcal{D}$ under the action of the γ-matrix. Consequently, we do not have here a topological invariant which may be equivalently computed in the fundamental domain and in its copy. This problem may be solved by using an unsigned fundamental linking number $\tilde{\mathcal{L}}(N_i, N_j) = \mid \mathcal{L}(N_i, N_j) \mid$ which mods out the dependence on the choice of the fundamental domain. No information is lost when we are working with such an unsigned linking number $\tilde{\mathcal{L}}$ since we have no prescription to choose between the positive and the negative signs. Indeed, due to the equivariance properties, to each oriented crossing between a fundamental orbit N_i and a fundamental orbit N_j on the fundamental domain is associated an oriented crossing on its copy but, as the inversion

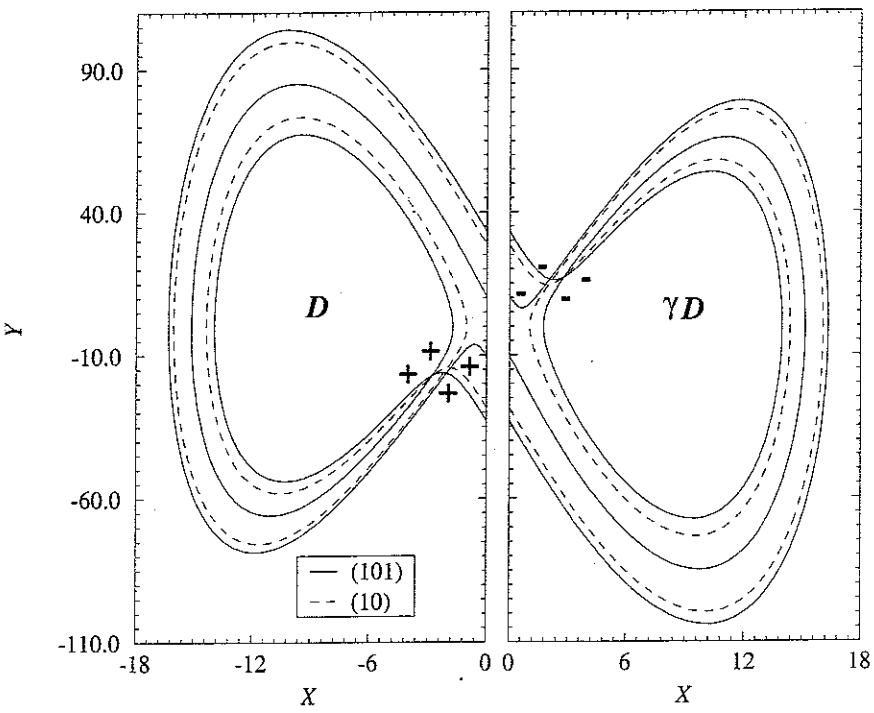

Fig. 12. — Plane projections of the fundamental orbit pair (101, 10) in the fundamental domain $\mathcal{D}$ and its copy $\gamma\mathcal{D}$. The fundamental linking numbers are found to be opposite but $\tilde{\mathcal{L}}(101,1) = \frac{1}{2}|+4| = 2$.

symmetry reverses the signs of crossings, a positive crossing in $\mathcal{D}$ is found to be negative on $\gamma\mathcal{D}$. In particular, on the x-induced attractor, all the positive crossings counted on $\mathcal{D}$ are counted as negative on $\gamma\mathcal{D}$.

For instance, let us determine the fundamental linking number between two couples of fundamental periodic orbits encoded by (101, 10) and (1, 100), respectively. The unsigned fundamental linking number $\tilde{\mathcal{L}}(101,10)$ is then found to be equal to 2 (Fig. 12) which is therefore equal (within the value of the sign) to the fundamental linking number $\mathcal{L}(101,10)$ obtained on the original Lorenz attractor (Fig. 8a). The unsigned fundamental linking number is then also in agreement with the template construction (Fig. 8b). Similarly, the unsigned fundamental linking number $\tilde{\mathcal{L}}(1,100)$ is found to be equal to 1 (Fig. 13) and may easily be checked by a construction on the original template. All unsigned fundamental linking numbers of fundamental orbits whose period is less than 5 have been found to be in agreement with the original fundamental template prediction.

3.4. Attractor Induced by an Invariant Variable. — The observable is now the invariant variable z. This variable contains no information about the symmetry and, consequently, the attractor reconstructed from this variable does not present any symmetry property. The reconstructed space is spanned by the set of coordinates $(X,Y,Z) = (z,\dot{z},\ddot{z})$. Thus the topological characterization of A_z is conducted following the procedure used for the Rössler system. This reconstructed attractor has a first-return map to the Poincaré set $P_Z = \{(Y,Z) \in \mathbb{R}^2 \mid X = 30, \dot{X} > 0\}$ which is similar to the original Lorenz map (Fig. 14).

As in the previous cases, the increasing branch is associated with a strip without any local torsion labelled by symbol 0, and the decreasing branch is associated with a strip with a π-twist and is labelled by symbol 1. Periodic orbits are extracted and encoded following this symbolic dynamics. Attractor A_z is a simply folded ribbon with a structure similar to the Rössler

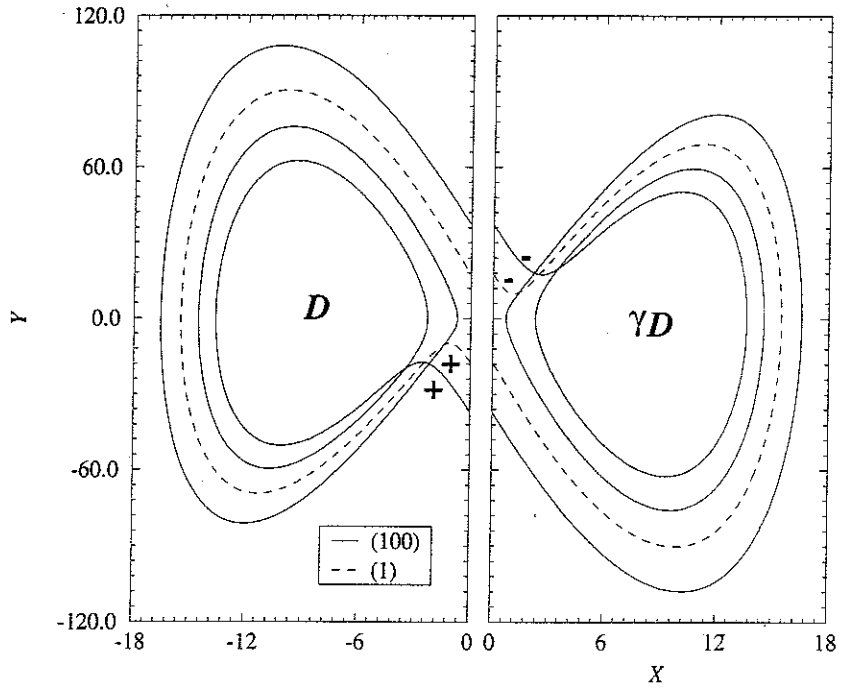

Fig. 13. — Plane projections of the fundamental orbit pair (1, 100) in the fundamental domain $\mathcal{D}$ and its copy. $\tilde{\mathcal{L}}(1,100) = \frac{1}{2}|+2| = 1$.

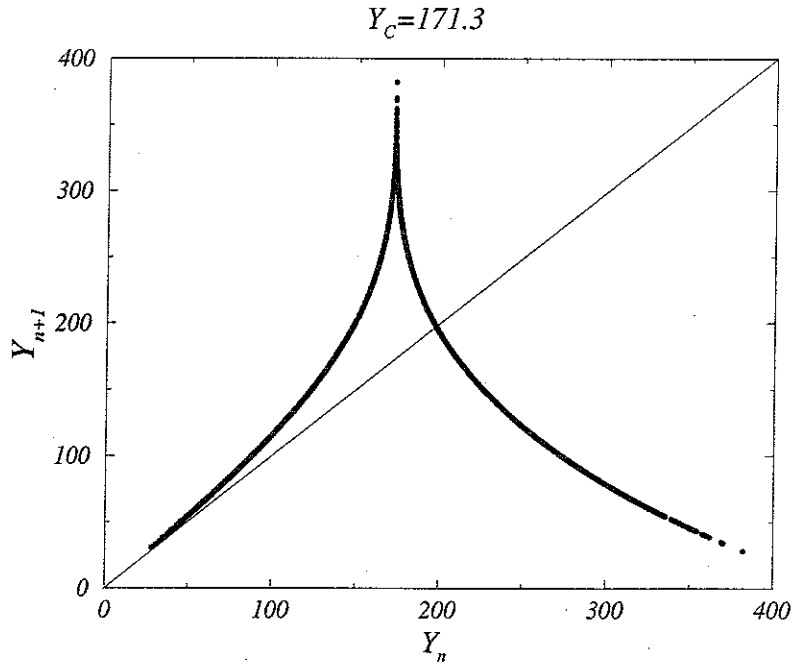

Fig. 14. — First-return map of the z-induced attractor.

attractor but with a positive local torsion. Its template may easily be found equivalent to the template of the fundamental domain of the Lorenz attractor. It is worthwhile emphasizing that this equivalence holds between a non fundamental template (template on the whole attractor A_z) and a fundamental template, pointing out once more the interest of the concept of restricted

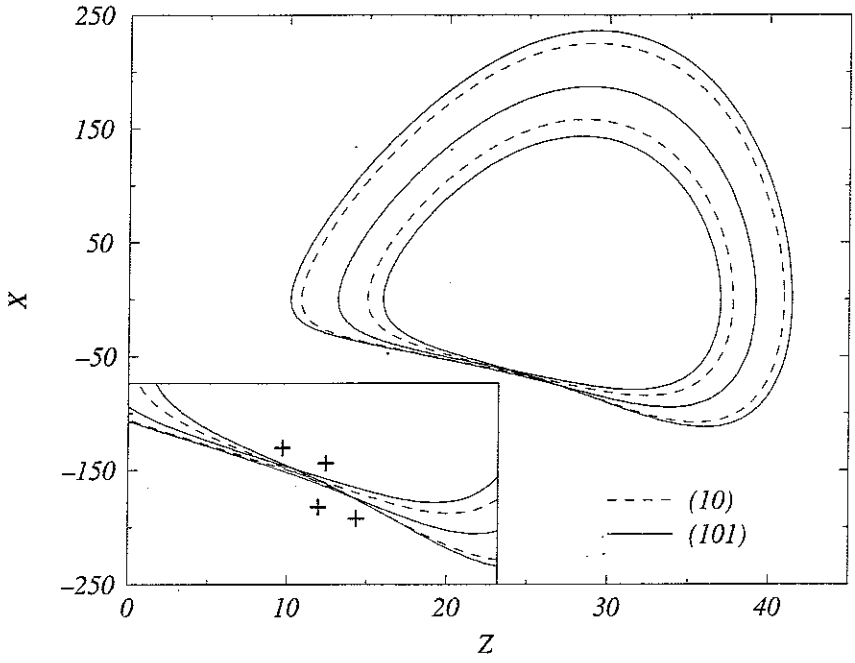

Fig. 15. — Plane projection of the orbit couple (101, 10) of A_z: $\mathrm{L}(101,10) = \frac{1}{2}(+4) = +2$.

topological equivalence.

Orbits encoded by (10) and (101) are displayed in Figure 15. The linking number $L(101,10)$ is given here by the half-sum of the oriented crossings, and is found to be equal to +2 as on the original attractor. The linking number is preserved and the reconstructed attractor is topologically equivalent (in the restricted sense) to the original one.

Indeed, the one wing attractor A_z may be viewed as an explicit representation of the fundamental domain $\mathcal{D}$ of the original Lorenz attractor, *i.e.* z-variable is a useful variable to analyse the dynamical behaviour of the Lorenz system. Naturally, information about symmetry properties is not available from this observable. Nevertheless let us note that this variable is always used to compute power spectra, first-return maps, ... We have shown the deep root of this common habit, *i.e.* z-time series contain information about dynamics projected on the fundamental domain $\mathcal{D}$ which is often implicitly used to analyse the Lorenz system.

Indeed it is well-known [40,41] that power spectra computed from the different variables of the Lorenz system are not equivalent (Fig. 16): power spectra from equivariant variables (x or y) provide no peak while the power spectrum from the invariant z-variable provides a peak at $f_0 = 1.30$ Hz.

Let us recall that when a power spectrum of a variable $w(t)$ is composed of sharp peaks superimposed on a broad background, the linearity of the Fourier transformation implies that $w(t)$ can be written as the sum of a periodic and a nonperiodic part:

$$w(t) = w_{\mathrm{p}}(t) \; + \; w_{\mathrm{np}}(t) \tag{27}$$

Consequently, power spectra of equivariant variables reveal that no periodic components are really present in these variables. Conversely, a principal frequency f_z equal to 1.30 Hz may be exhibited from the power spectrum of the invariant z-variable (Fig. 16). This implies that a phase coherence [40] appears on the fundamental domain (remember that the invariant z-variable naturally projects the dynamics on the fundamental domain). In other words, a

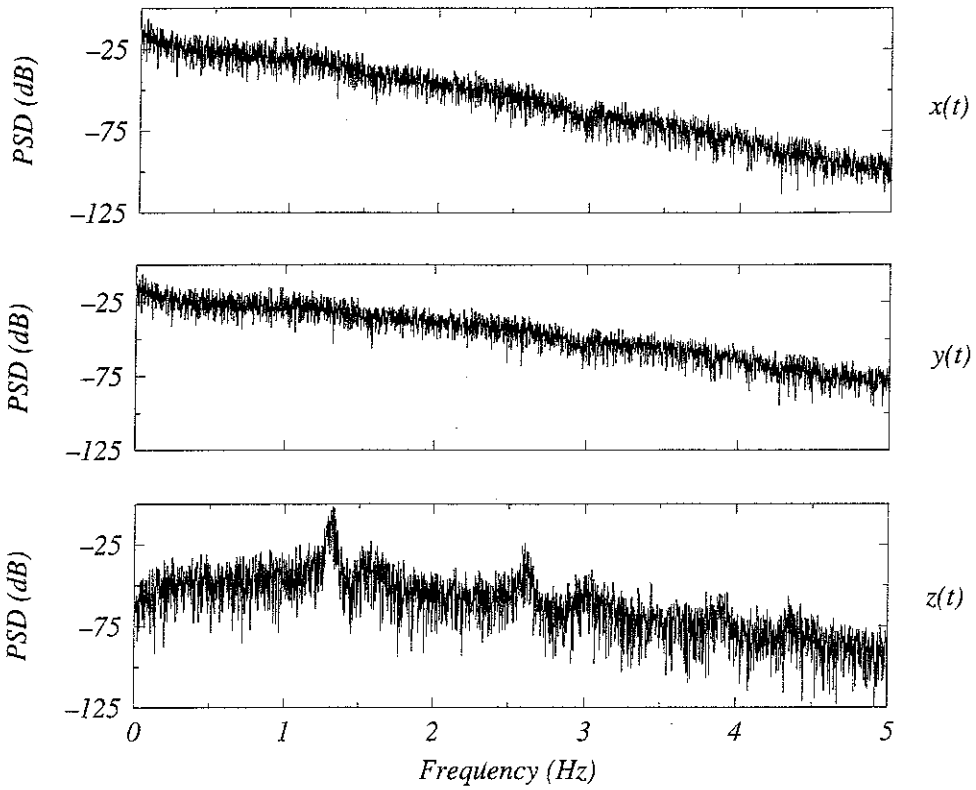

Fig. 16. — Power spectra of the different variables of the Lorenz system. Equivariant variable provide no peak while the invariant variable provide a peak at 1.30 Hz.

significant pseudo-period may be defined by the average time between two consecutive intersections with a Poincaré section P_y in a fundamental domain of the original attractor. We found such a pseudo-period to be $T_0 = 0.75 \pm 0.10$ s in very good agreement with the one estimated from the power spectrum of z: $T_z \approx 0.76$ s. The invariant z-observable provides therefore pertinent dynamical information on the Lorenz dynamics.

Imagine now that the y-time series is recorded. One may easily check that the observable y is equivariant in a simple way, *i.e.* that its time series is globally invariant by multiplying by -1 (this requires a prior reconstruction of the strange attractor to detect the equivariance). Consequently, we know that the original attractor may be tasselated by a fundamental domain $\mathcal{D}$ and one of its copy $\gamma\mathcal{D}$. Even if we do not know whether the symmetry is of the axial or inversion type, we may safely use the absolute value of the time series to compute the power spectrum and find the representative frequency of the original system. If this is carried out with the y-time series of the Lorenz system, then the power spectrum of $|y|$ presents a peak at 1.31 Hz which is in good agreement with the pseudo-period T_0 exhibited on the fundamental domain $\mathcal{D}$ (Fig. 17). Let us note that we might similarly use y^2 instead of $|y|$.

4. Conclusion

We investigated the topological characterization of reconstructed attractors in the case of 3D-embeddings. The reconstruction technique used relies on derivative coordinates but our conclusions extend to other kinds of embedding. We focused our attention on the case of equivariant systems and developed a specific topological characterization modding out symmetries leading to the concept of restricted topological equivalence when the analysis is performed on

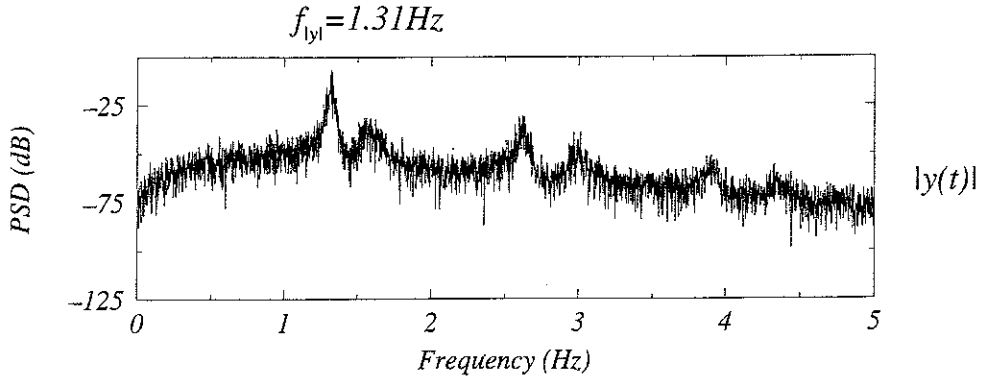

Fig. 17. — Power spectrum of the absolute values of the y-time series of the Lorenz system. A principal peak is recovered at the same frequency than on the power spectra of z.

a fundamental domain. Relying on specific examples, we demonstrated that restricted topological equivalence between original and reconstructed attractors may hold even if topological equivalence in the strict sense does not hold. Our results confirm the importance of the topological properties in the analysis of dynamical systems. For experimental cases however, it may be difficult to state if the reconstructed portrait is correct or not. Therefore, detecting pathological topology, such as symmetry or "8"-configuration, in experimental systems appears as a topic of great interest (in detecting the symmetry, see [42]).

Acknowledgments

We are indebted to anonymous reviewers for their extremely helpful recommendations. In particular, one of them allowed us to explicitly introduce the concept of restricted topological equivariance which considerably clarifies the discussion. Such a clarification which is not only a matter of terminology is not available in reference [35]. Another reviewer helped us to further clarify the discussion by introducing some concepts in a simpler way than in the original version of the manuscript. We wish to thank D. Moscato for the helpful English corrections of the manuscript.

References

[1] Packard N.H., Crutchfield J.P., Farmer J.D. and Shaw R.S., *Phys. Rev. Lett.* **45** (1980) 712-716.
[2] Broomhead D.S. and King G.P., *Physica D* **20** (1986) 217-236.
[3] Gibson J.F., Farmer J.D., Casdagli M. and Eubank S., *Physica D* **57** (1992) 1-30.
[4] Mindlin G.B. and Gilmore R., *Physica D* **58** (1992) 229-242.
[5] Agarwal A.K., Ahalpara D.P., Kaw P.K., Prablakera H.R. and Sen A., *J. Phys.* **35** (1990) 287-301.
[6] Breeden J.L. and Hübler A., *Phys. Rev. A* **42** (1990) 5817-5826.
[7] Gouesbet G., *Phys. Rev. A* **43** (1991) 5321-5331.
[8] Gouesbet G., *Phys. Rev. A* **44** (1991) 6264-6280.
[9] Gouesbet G., *Phys. Rev. A* **46** (1992) 1784-1796.
[10] Gouesbet G. and Maquet J., *Physica D* **58** (1992) 202-215.
[11] Brown R., Rulkov N.F. and Tracy E.R., *Phys. Rev. E* **49** (1994) 3784-3800.
[12] Palus M. and Dvoràck I., *Physica D* **55** (1992) 221-234.

[13] Casdagli M., Eubank S., Farmer J.D. and Gibson J., *Physica D* **51** (1991) 52-98.
[14] Gouesbet G. and Letellier C., *Phys. Rev. E* **49** (1994) 4955-4972.
[15] Takens F., "Detecting Strange Attractors in Turbulence", in: Dynamical Systems and Turbulence, Warwick 1980, Lecture Notes in Mathematics, Vol. 898, D.A. Rand and L.S. Young Eds., vol. 898 (Springer-Verlag, New York, 1981) pp. 366-381.
[16] Buzug Th. and Pfister G., *Phys. Rev. A* **45** (1992) 7073-7984.
[17] Abarbanel H.D.I. and Kennel M.B., *Phys. Rev. E* **47** (1993) 3057-3068.
[18] Abarbanel H.D.I., Brown R., Sidorowich J.J. and Tsimring L.Sh., *Rev. Modern Phys.* **65** (1993) 1331-1388.
[19] Lorenz E.N., *J. Atmospheric Sci.* **20** (1963) 130-141.
[20] Letellier C., Ringuet E., Maheu B., Maquet J. and Gouesbet G., "Global vector field reconstruction of chaotic attractors from one unstable periodic orbit", Actes des 4èmes Journées Européennes de Thermodynamique, Nancy, France, les 27-29 Septembre 1995, pp. 459-469 to be published in *Entropie*.
[21] Sauer T., Yorke J. and Casdagli M., *J. Stat. Phys.* **65** (1991) 579-616.
[22] Gershenfeld N., "An Experimentalist's Introduction to the Observation of Dynamical Systems", in Directions in Chaos, Hao Bai Lin Ed., Vol. 2 (World Scientific Publishing, Singapore, 1988) pp. 310-384.
[23] Demazure M., Catastrophes et Bifurcations (Ellipse, Paris, 1989).
[24] Rössler O.E., *Physics A Lett.* **57** (1976) 397-398.
[25] Mindlin G.B., Hou X.J., Solari H.G., Gilmore R. and Tufillaro N.B., *Phys. Rev. Lett.* **64** (1990) 2350-2353.
[26] Politi A., From Statistical Physics to Statistical Inference and Back, P. Grassberger and J.P. Nadal Eds. (Kluwer Acad. Pub Boston, 1994).
[27] Tufillaro N.B., From Statistical Physics to Statistical Inference and Back, P. Grassberger and J.P. Nadal Eds. (Kluwer Acad. Pub Boston, 1994).
[28] Tufillaro N.B., Wyckoff P., Brown R., Schreiber T. and Molteno T., *Phys. Rev. E* **51** (1995) 164-174.
[29] Letellier C., Dutertre P. and Maheu B., *Chaos* **5** (1995) 272-281.
[30] Melvin P. and Tufillaro N.B., *Phys. Rev. A* **44** (1991) 3419-3422.
[31] Tufillaro N.B., Abbott T. and Reilly J., An Experimental Approach to Nonlinear Dynamics and Chaos (Addison-Wesley, New York, 1992).
[32] Mindlin G.B., Solari H.G., Natiello M.A., Gilmore R. and Hou X.J., *J. Nonlinear Sci.* **1** (1991) 147-173.
[33] Letellier C., Caractérisation topologique et reconstruction d'attracteurs étranges, PhD dissertation, CORIA, LESP, Rouen, France (1994).
[34] King G.P. and Stewart I., *Physica D* **58** (1992) 216-228.
[35] Cvitanović P. and Eckhardt B., *Nonlinearity* **6** (1993) 277-311.
[36] Letellier C., Dutertre P. and Gouesbet G., *Phys. Rev. E* **49** (1994) 3492-3495.
[37] Birman J.S. and Williams R.F., *Topology* **22** (1983) 47-82.
[38] Sparrow C., "The Lorenz Equations: Bifurcations, Chaos and Strange Attractors", Applied Mathematical Sciences, Vol. 41 (Springer-Verlag, Berlin, 1982).
[39] The template here considered differs from the two-branch template considered by Birman and Williams in that it is not a braid template.
[40] Farmer J.D., Crutchfield J.P., Frœling H., Packard N.H. and Shaw R.S., *Annals N.Y. Acad. Sci.* **357** (1980) 453-472.
[41] Hao Bai Lin, Elementary Symbolic Dynamics and Chaos in Dissipative Systems (World Scientific Publishing, Singapore, 1989).
[42] Barany E., Delinitz M. and Golubitsky M., *Physica D* **67** (1993) 66-87.